Int. J. Heat Mass Transfer. Vol. 30, No. 9, pp. 1927–1939, 1987
Printed in Great Britain

0017-9310/87 $3.00 + 0.00
Pergamon Journals Ltd.

Drift flux model for large diameter pipe and new correlation for pool void fraction

ISAO KATAOKA
Institute of Atomic Energy, Kyoto University, Uji, Kyoto 611, Japan

and

MAMORU ISHII†
Reactor Analysis and Safety Division, Argonne National Laboratory, 9700 South Cass Avenue, Argonne, IL 60439, U.S.A.

(*Received* 23 *October* 1986 *and in final form* 16 *February* 1987)

Abstract—A void fraction for a bubbling or boiling pool system is one of the important parameters in analyzing heat and mass transfer processes. Using the drift flux formulation, correlations for the pool void fraction have been developed in comparison with a large number of experimental data. It has been found that the drift velocity in a pool system depends upon vessel diameter, system pressure, gas flux and fluid physical properties. The results show that the relative velocity and void fraction can be quite different from those predicted by conventional correlations. In terms of the rise velocity, four different regimes are identified. These are bubbly, churn-turbulent, slug and cap bubble regimes. The present correlations are shown to agree with the experimental data over a wide range of parameters such as vessel diameter, system pressure, gas flux and physical properties.

1. INTRODUCTION

WHEN GAS is injected into stagnant liquid or boiling occurs in a pool of liquid, two characteristic phenomena can be observed. One is the entrainment of liquid droplets from a free surface of a liquid pool. Another is the liquid level swelling due to the void created by the vapor volume in a liquid pool. Both phenomena are important in heat and mass transfer processes utilizing bubbling or pool boiling. For the pool entrainment phenomenon, a reliable correlation has recently been developed based on the detailed mechanistic modeling [1]. The entrainment amount is correlated in terms of a gas flow rate and the distance from the free surface of a liquid pool.

The liquid level, H, in a bubbling or pool boiling system can be given in terms of an average pool void fraction, α, as

$$H = \frac{H_0}{1-\alpha}. \tag{1}$$

Here H_0 is the liquid level without void or the collapsed level of the pool. Therefore, the pool void fraction is one of the most important parameters characterizing a bubbling or pool boiling system.

Recently, the importance of accurately predicting the pool void fraction has been recognized in relation to safety analyses of nuclear reactors. For example, in case of a pump trip during a small break LOCA (loss of coolant accident), such as the TMI accident, or in a reflooding phase of a large break LOCA, the inlet flow rate to the reactor core can be rather small. Due to the decay heat from fuel rods, boiling occurs in the almost stagnant liquid in the core. In these cases, a prediction of the liquid level in a reactor core is quite important in terms of safety evaluations. Below the liquid level fuel rods can be cooled sufficiently while above it they can be heated up considerably. Therefore, for accurate predictions of the maximum cladding temperature, knowledge of the pool void fraction is indispensable. There have been several correlations for the pool void fraction. However, they are not necessarily applicable to a whole range of operational parameters of practical importance. In view of this a correlation for the pool void fraction has been developed based on the drift flux formulation of two-phase flow in this study with particular emphasis on large vessel diameter and high gas flux range. In bubbling or pool boiling systems the ratio of the vessel diameter to the length is often large in comparison with forced convection systems. It is noted that a recirculation flow pattern may develop in a large vessel at low flow. This may significantly affect the transverse velocity and void fraction profiles. Therefore, the effect of the vessel diameter on the drift velocity has been carefully examined in detail. The obtained correlation is shown to predict accurately the pool void fraction over wide ranges of vessel diameters, vapor flow rates and pressures for various fluids.

† Author to whom all correspondence should be addressed.

NOMENCLATURE

A_p	parameter in equation (29)
C_0	distribution parameter
C_D	drag coefficient of bubble in two-phase media
$C_{D\infty}$	drag coefficient of bubble in infinite liquid
D_H	hydraulic diameter of vessel
D_H^*	dimensionless hydraulic diameter, $D_H/\sqrt{(\sigma/g\Delta\rho)}$
$f(x)$	function of x
g	acceleration due to gravity
H	liquid level
H_0	liquid level without void (collapsed level)
j	total flux of gas and liquid
j_f	liquid flux (superficial velocity of liquid)
j_g	gas flux (superficial velocity of gas)
j_g^*	dimensionless gas flux, $j_g/(\sigma g\Delta\rho/\rho_g^2)^{0.25}$
j_g^+	dimensionless gas flux, $j_g/(\sigma g\Delta\rho/\rho_f^2)^{0.25}$
$N_{\mu f}$	viscosity number, $\mu_f/(\rho_f\sigma\sqrt{(\sigma/g\Delta\rho)})^{0.5}$
P	system pressure
r	radial position of vessel
R	radius of vessel
u_f	velocity of liquid phase
u_g	velocity of gas phase
V_{gj}	drift velocity
V_{gj}^+	dimensionless drift velocity, $\langle\langle V_{gj}\rangle\rangle/(\sigma g\Delta\rho/\rho_f^2)^{0.25}$
$V_{gj\text{loc}}$	local drift velocity
$V_{gj\infty}$	drift velocity in infinite liquid
$\langle\langle V_{gj}\rangle\rangle$	void weighted, area averaged local drift velocity, $\int \alpha V_{gj}\,dA/\int \alpha\,dA$
x	gas or vapor quality.

Greek symbols

α	void fraction
α_{loc}	local void fraction
μ_f	viscosity of liquid
ρ_f	density of liquid
ρ_g	density of gas
$\Delta\rho$	density difference between gas and liquid
σ	surface tension.

2. PREVIOUS WORK

2.1. *Different approaches*

The standard void-quality correlations which are often used in forced convection two-phase flow analyses are almost useless in predicting the pool void fraction. This is explained below. These correlations are given in a form of

$$\alpha = f(x). \tag{2}$$

Here x is the quality of the gas phase defined by

$$x = \frac{\rho_g j_g}{\rho_g j_g + \rho_f j_f} \tag{3}$$

where ρ and j are the density and volumetric flux. Subscripts g and f denote the gas and the liquid, respectively. For a bubbling or pool boiling system, the liquid flux is almost zero, that is $j_f \simeq 0$. Then equation (3) implies $x \simeq 1$, regardless of gas flux. Therefore, equation (2) does not give any knowledge of the pool void fraction.

Two different approaches may be used in developing a practical pool void fraction correlation. The first one is to develop a purely empirical correlation in terms of several dimensionless groups. The second approach is to use a two-phase flow model such as the drift flux model [2–5] or two-fluid model [6–8]. In the latter approach, the constitutive relations for the relative motion and phase distribution are necessary for the development of a void fraction correlation. In general, the drift flux model is simpler and more convenient for this correlation development purpose than the two-fluid model.

In what follows, previous studies on pool void fraction correlations are reviewed according to the above-mentioned categories.

2.2. *Empirical correlations*

Empirical correlations for the pool void fraction are usually expressed in terms of some powers of several dimensionless groups. The early attempts have been carried out by Russian researchers. These are summarized by Yeh and Zuber [9]. Among these early works, the ones developed by Sterman [10] and Dimentiev *et al.* [11] are representative and given by

$$\alpha = 1.07 j_g^{*0.8} D_H^{*-0.25}\left(\frac{\rho_g}{\Delta\rho}\right)^{-0.23} \quad \text{for} \quad j_g^*\left(\frac{\rho_g}{\Delta\rho}\right)^{-1/2} \leqslant 3.7 \tag{4}$$

and

$$\alpha = 1.9 j_g^{*0.34} D_H^{*-0.25}\left(\frac{\rho_g}{\Delta\rho}\right)^{0.09} \quad \text{for} \quad j_g^*\left(\frac{\rho_g}{\Delta\rho}\right)^{-1/2} \geqslant 3.7. \tag{5}$$

Here j_g^* and D_H^* are defined by

$$j_g^* \equiv j_g \Big/ \left(\frac{\sigma g\Delta\rho}{\rho_g^2}\right)^{1/4} \tag{6}$$

$$D_H^* \equiv D_H \Big/ \sqrt{\left(\frac{\sigma}{g\Delta\rho}\right)} \tag{7}$$

where σ, g, $\Delta\rho$ and D_H are the surface tension, accel-

eration due to gravity, density difference between liquid and gas and hydraulic diameter of a vessel. Equations (4) and (5) are developed from experimental data for steam–water. For large vessel diameters, Sterman [12] proposed another correlation instead of equation (4). It is given by

$$\alpha = 0.26 j_g^{*0.8} \left(\frac{\rho_g}{\Delta\rho}\right)^{-0.28} \quad \text{for} \quad D_H^* \left(\frac{\rho_g}{\Delta\rho}\right)^{-0.2} \geqslant 260. \quad (8)$$

Wilson *et al.* [13, 14] modified the above correlation based on their own experimental data. It is given by

$$\alpha = 0.68 j_g^{*0.62} D_H^{*-0.1} \left(\frac{\rho_g}{\Delta\rho}\right)^{-0.14} \quad \text{for} \quad j_g^* \left(\frac{\rho_g}{\Delta\rho}\right)^{-1/2} \leqslant 2 \quad (9)$$

$$\alpha = 0.88 j_g^{*0.4} D_H^{*-0.1} \left(\frac{\rho_g}{\Delta\rho}\right)^{-0.03} \quad \text{for} \quad j_g^* \left(\frac{\rho_g}{\Delta\rho}\right)^{-1/2} \geqslant 2. \quad (10)$$

Later, Bartolomei and Alkhuton [15] and Sudo [16] proposed correlations in this category using additional dimensionless parameters.

These empirical power law correlations are easy to develop. However, one of the main difficulties of these correlations is their inconsistency with void correlations for forced convection systems. In many engineering problems it is necessary to calculate the void fractions continuously over a wide range of flow conditions. In these cases, the above discrepancy may lead to artificial discontinuities or numerical problems. In safety evaluations of nuclear reactor accidents, a wide range of the liquid flux must be considered and thus the void correlation should be applicable to both pool and forced convection conditions. For this purpose, the above-mentioned correlations may become inappropriate. The main reason for this shortcoming is that these correlations were developed purely empirically from data limited to a particular flow condition and they were not based on physical modeling of two-phase flow.

2.3. *Drift flux type correlations*

The drift flux model [2–5] is one of the most practical and accurate models for two-phase flow. The model takes into account the relative motion between phases by a constitutive relation. It has been utilized to solve many engineering problems involving two-phase flow dynamics. In particular, its applications to forced convection systems have been quite successful. In the one-dimensional drift flux model [2–4] the relative velocity v_r is given by

$$(1-\alpha)v_r = (C_0 - 1)j + \langle\langle V_{gj} \rangle\rangle \quad (11)$$

where C_0, j and $\langle\langle V_{gj} \rangle\rangle$ are the distribution parameter, total volumetric flux and α weighted area average of the local drift velocity, respectively. The first term on the right-hand side of equation (11) represents the difference between the average phase velocities arising from the void and velocity profiles, whereas the second term represents the average effect of the local slip between the phases.

By definition, the total volumetric flux and relative velocity are given by

$$j = j_g + j_f \quad (12)$$

and

$$v_r = u_g - u_f. \quad (13)$$

Here the average velocities of gas and liquid can be related to the volumetric fluxes by

$$u_g = j_g/\alpha \quad (14)$$

$$u_f = j_f/(1-\alpha).$$

Using the above relations the void fraction can be given by

$$\alpha = \frac{j_g}{C_0 j + \langle\langle V_{gj} \rangle\rangle}. \quad (15)$$

According to Ishii [3], C_0 for a round tube in the moderate Reynolds number range is given by

$$C_0 = 1.2 - 0.2\sqrt{\left(\frac{\rho_g}{\rho_f}\right)} \quad (16)$$

and for a rectangular channel by

$$C_0 = 1.35 - 0.35\sqrt{\left(\frac{\rho_g}{\rho_f}\right)}. \quad (17)$$

For very low or high Reynolds number flows, some modifications are necessary [3].

On the other hand, $\langle\langle V_{gj} \rangle\rangle$ is the average local drift velocity which accounts for the local velocity difference between gas and liquid. Ishii [3] proposed constitutive relations for the local drift velocity in various two-phase flow regimes.

Bubbly flow

$$\langle\langle V_{gj} \rangle\rangle = \sqrt{2}\left(\frac{\sigma g \Delta\rho}{\rho_f^2}\right)^{1/4} (1-\alpha)^{7/4}. \quad (18)$$

Churn turbulent bubbly flow

$$\langle\langle V_{gj} \rangle\rangle = \sqrt{2}\left(\frac{\sigma g \Delta\rho}{\rho_f^2}\right)^{1/4}. \quad (19)$$

Slug flow

$$\langle\langle V_{gj} \rangle\rangle = 0.35\sqrt{\left(gD_H\left(\frac{\Delta\rho}{\rho_f}\right)\right)}. \quad (20)$$

Using the expression given by the above constitutive

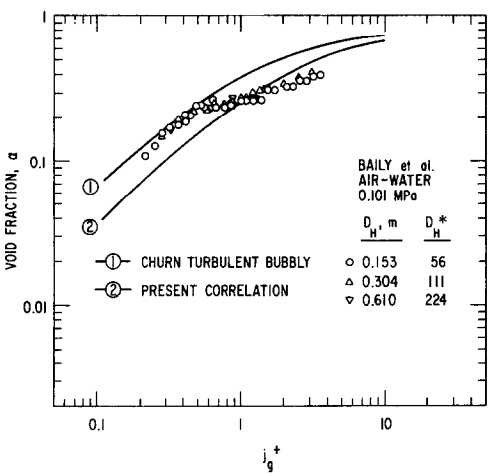

FIG. 1. Comparison of experimental pool void fraction of Baily *et al.* [17] with values predicted by equation (22) with equation (19) (churn turbulent bubbly) and equation (35) (present correlation).

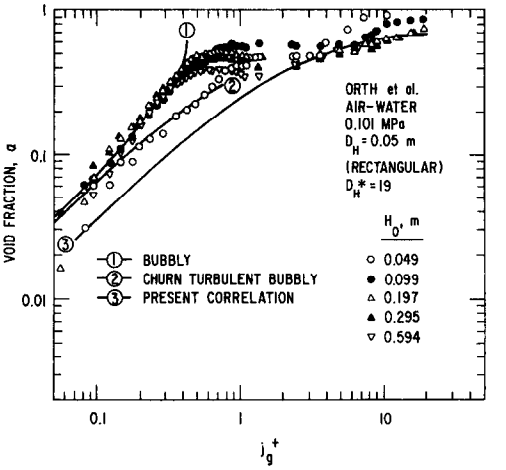

FIG. 2. Comparison of experimental pool void fraction of Orth [18] with values predicted by equation (22) with equation (18) (bubbly), equation (19) (churn turbulent bubbly) and equation (35) (present correlation).

relations, the void fraction can be predicted reasonably well for a forced convection system with a relatively small hydraulic diameter ($D_H \leqslant 40/\sqrt{(\sigma/g\Delta\rho)}$).

This type of correlation has the advantage of possible applicability to pool void fraction. For bubbling or pool boiling, liquid flux is zero. Then

$$j = j_g. \tag{21}$$

Substituting equation (21) into equation (13) one obtains

$$\alpha = \frac{j_g}{C_0 j_g + \langle\langle V_{gj} \rangle\rangle}. \tag{22}$$

Equation (22), together with equations (15), (16) and (18)–(20), gives a prediction of pool void fraction. Actually, for small j_g this correlation predicts pool void fraction very well [2, 5]. In view of equations (18), (19) and (22), one introduces another dimensionless gas flux, j_g^+, which is given by

$$j_g^+ \equiv j_g \Big/ \left(\frac{\sigma g \Delta\rho}{\rho_f^2}\right)^{1/4}. \tag{23}$$

This is related to j_g^* which is given by equation (8) as

$$j_g^+ = j_g^* \left(\frac{\rho_g}{\rho_f}\right)^{1/2}. \tag{24}$$

Figure 1 shows one example. As pointed out by Zuber and Findlay [2], for small j_g^+ where

$$j_g^+ \leqslant 0.5 \tag{25}$$

the experimental data of pool void fraction of Baily *et al.* [17] are well predicted by equation (22) with drift velocity for churn turbulent bubbly flow, equation (19).

Figure 2 shows the experimental data of the pool void fraction of Orth [18]. In his experiment collapsed liquid levels (liquid level without void), H_0, are varied. In this case, equation (22), with drift velocity for bubbly flow, equation (18), can predict the experimental data well for small j_g^+ which is given by $j_g^+ \leqslant 0.4$ for $H_0 \leqslant 9.9$ cm. On the other hand, for small H_0 (4.9 cm), the pool void fraction is predicted by equation (22) with equation (19) (churn turbulent bubbly flow).

Thus, for small j_g^+ (approximately up to 0.5), the pool void fraction can be predicted by a drift flux type correlation, equation (22), with drift velocity for bubbly flow or churn turbulent bubbly flow. The flow regime (bubbly flow or churn turbulent bubbly flow) depends on how the gas is injected (Zuber and Hench [19]), liquid impurity (Wallis [20]) and collapsed level (Fig. 2, Orth [18]). However, for larger j_g given by $j_g^+ \gtrsim 0.5$, previous drift flux type correlation, equation (22) with equations (18)–(20), shows considerable discrepancies with experimental data, particularly for large diameter vessels.

Visual observations indicate that in the range of $j_g^+ > 0.5$, large slug bubbles or cap like bubbles appear together with highly deformed small bubbles [16, 21]. Therefore, the drift velocities for churn turbulent flow, equation (19), or for slug flow, equation (20), are assumed to be more applicable. Figure 3 is an example of the comparison of experimental data with equation (22) with equations (19) and (20).

Figure 3 shows the experimental data for air–water at atmospheric pressure for various vessel diameters [16]. As shown in this figure, the drift flux type correlation, equation (22), with slug flow drift velocity, equation (20), is applicable only for small diameter ($D_H = 2.2$ cm). For other diameters, the correlation does not show good agreement with experimental data. Neither churn turbulent flow drift velocity, equation (19), predicts the experimental data for various diameters. Actually, visual observation [16] reveals that for the smallest vessel diameter ($D_H = 2.2$ cm) ideal shaped slug bubbles appear whereas for larger diameters, large bubbles are too deformed

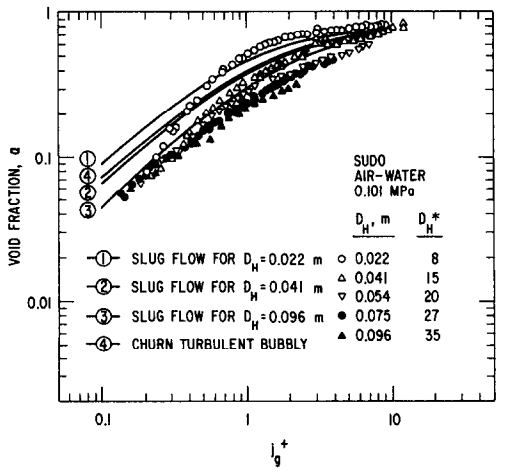

FIG. 3. Comparison of experimental pool void fraction of Sudo [16] with values predicted by equation (22) with equation (20) (slug) and equation (19) (churn turbulent bubbly).

to be called 'slug bubbles'. The disagreement of drift velocity for slug flow, equation (20), with experimental data can be attributed to this deformation.

Furthermore, the experimental data for steam–water at various pressures in a large diameter vessel ($D_H = 0.456$ m) [22] show that neither the slug flow drift velocity, equation (20), nor the churn turbulent drift velocity, equation (19), predict the experimental data well. This discrepancy between the previous drift flux type correlations and experimental data are seen for all available data for pool void fraction as listed in Table 1.

Earlier, Zuber and Findlay [2] pointed out this discrepancy. They assumed that the flow regime for pool bubbling or boiling is different from that for forced convection. They called this flow regime the 'Pseudo-jet Flow Regime' and assigned the drift velocity different from that for forced convection. Based on the mechanism that large bubbles or jets are produced from nozzles or perforations, they proposed a pool void fraction correlation which is given by

$$\alpha = \frac{1}{C_0 + A_p/j_g^*}. \tag{26}$$

Here A_p is constant but system dependent. The drift velocity is then given by

$$\langle\langle V_{gj}\rangle\rangle = A_p \left(\frac{\sigma g \Delta\rho}{\rho_g^2}\right)^{1/4}. \tag{27}$$

They have shown appropriate values of A_p for several experimental data [13, 14, 22–24] but correlation for A_p has not been presented. A similar approach has been carried out by Labuntov *et al.* [25].

Although it was dimensional and empirical, Filimonov *et al.* [23], correlated steam–water data mainly in the U.S.S.R. by drift flux type correlation. In their correlation, C_0 in equation (22) is approximated by unity, that is, $C_0 = 1$. Then the drift velocity is given by

$$\langle\langle V_{gj}\rangle\rangle = (0.65 - 0.0385P)\left(\frac{D_H}{0.063}\right)^{0.25} \quad \text{for} \quad P = 1.1\text{–}12.7\,\text{MPa}$$
$$\langle\langle V_{gj}\rangle\rangle = (0.33 - 0.00133P)\left(\frac{D_H}{0.063}\right)^{0.25} \quad \text{for} \quad P = 12.7\text{–}18.2\,\text{MPa} \tag{28}$$

where $\langle\langle V_{gj}\rangle\rangle$ is in meters per second, P is the system pressure (MPa) and D_H is in meters.

As shown above, a drift flux type correlation is promising in correlating pool void fraction. However, the drift velocity has not yet been established. In particular, the effects of vessel diameter and pressure are important and they should be included in a correlation.

In view of this, in what follows, the drift velocity for bubbling or pool boiling is examined in detail and correlation for the drift velocity is developed based on a large number of experimental data now available. Special attention is focused on the effect of vessel

Table 1. Summary of various experiments on pool void fraction

Reference	Fluid	Vessel diameter, D_H (m)	Pressure (MPa)
Sudo [16]	air–water	0.022–0.096	0.101
Baily *et al.* [17]	air–water	0.153–0.610	0.101
Orth [18]	air–water	0.051 (rectangular)	0.101
Smissaert [28]	air–water	0.07	0.101
Ellis and Jones [27]	air–water	0.011–0.305	0.101
Yamaguchi and Yamazaki [21]	air–water	0.04–0.08	0.101
Petukhov and Kolokoltsen [29]	air–water air–glyceline	0.100 (rectangular)	0.1–2.5
Filimonov *et al.* [23]	steam–water	0.063	1.72–18.2
Wilson *et al.* [13, 14]	steam–water	0.102–0.48	1.03–4.14
Styrikovich *et al.* [24]	steam–water	0.238	0.61–9.32
Carrier *et al.* [22]	steam–water	0.456	4.1–13.8
Mochan *et al.* [35]	steam–water	0.030–0.076	1.22
Behringer [34]	steam–water	0.063	0.11–4.1

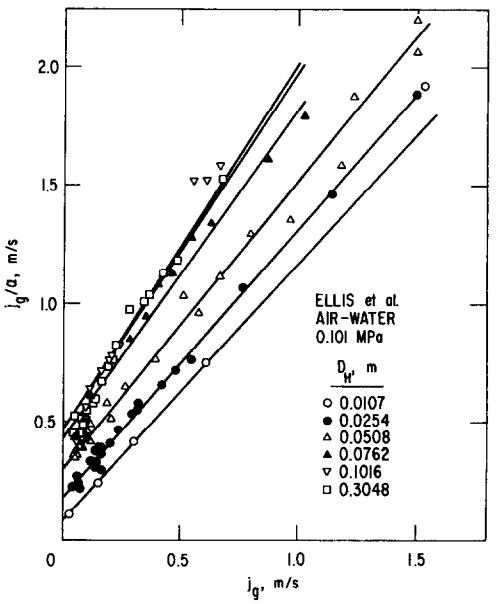

FIG. 4. Experimental data of Ellis and Jones [27] in the j_g vs j_g/α plane.

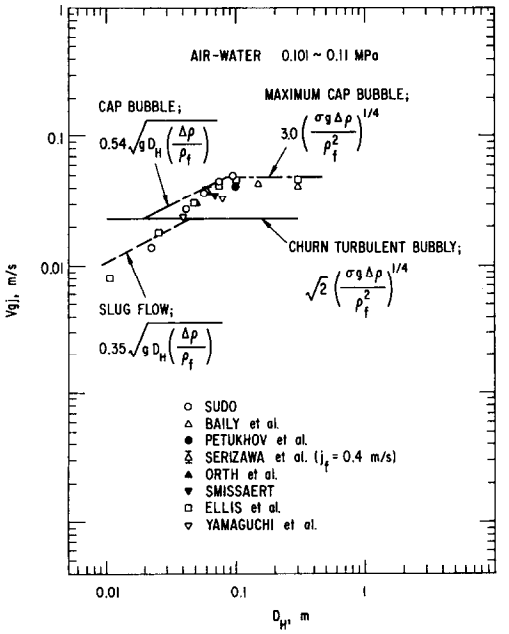

FIG. 5. Effect of vessel diameter on drift velocity obtained from air–water data.

diameter because in bubbling and pool boiling systems, vessel diameter varies widely and up to a considerable value.

3. DRIFT VELOCITY IN POOL

3.1. *Effect of vessel diameter on drift velocity*

First, the effect of vessel diameter on drift velocity is examined. For this purpose, the air–water test data at atmospheric pressure are appropriate. There are a large number of experimental data available (Table 1) where the vessel diameter is widely varied.

Figure 4 shows one example of the experimental data of the pool void fraction for air–water at atmospheric pressure with the vessel diameter ranging from 1.1 to 30 cm [26]. The data are shown in the j_g vs j_g/α plane. The j_g/α value at $j_g = 0$ represents the drift velocity if the distribution parameter C_0 is assumed to be constant. As shown in this figure, the drift velocity increases with the vessel diameter up to about 0.1 m and almost stays constant for a vessel diameter greater than 0.1 m. This tendency of experimental data has been examined in detail in ref. [26].

This tendency can be seen more clearly in Fig. 5 where the drift velocity is plotted as a function of the vessel diameter, D_H. In this figure, the drift velocity for slug flow, equation (20), and that for churn turbulent bubbly flow, equation (19), are shown. As can be seen in this figure, the drift velocity increases with D_H up to $D_H = 0.1$ m and levels off for $D_H \geq 0.1$ m.

Another characteristic feature of this figure is that the drift velocity agrees with that for slug flow, equation (20), for smaller vessel diameter ($D_H \leq 0.04$ m) whereas for $D_H \geq 0.04$ m, the drift velocity does not agree with either slug flow, equation (20), or churn turbulent bubbly flow, equation (19).

Recently, Ishii and Kocamustafaogullari [30] developed a theoretical correlation of drift velocity for cap bubble flow inside a large diameter channel. It is given by

$$V_{gj} = 0.54\sqrt{\left(gD_H\left(\frac{\Delta\rho}{\rho_f}\right)\right)} \quad \text{for} \quad D_H^* \leq 30 \tag{29}$$

$$V_{gj} = 3.0\left(\frac{\sigma g\Delta\rho}{\rho_f^2}\right)^{1/4} \quad \text{for} \quad D_H^* \geq 30. \tag{30}$$

In Fig. 5, the drift velocities for a cap bubble, equations (29) and (30), are also shown. Experimental data agree with cap bubble drift velocity for a larger vessel diameter. (For air–water at atmospheric pressure $D_H^* = 30$ corresponds to $D_H = 0.09$ m.)

The drift velocities obtained by experimental data, as shown in Fig. 5, are the 'averaged' values over the vessel area [2, 3] given by

$$V_{gj} = \frac{\int_0^{D_H/2} V_{gj|loc}\alpha_{loc}2\pi r\,dr}{\int_0^{D_H/2} \alpha_{loc}2\pi r\,dr}. \tag{31}$$

Here $V_{gj|loc}$ and α_{loc} are local values of drift velocity and void fraction in the radial position. Furthermore, V_{gj}, obtained in Fig. 5, is determined indirectly from the relation between j_g and j_g/α. Then a question arises. Do large bubbles in large diameter vessels really have large drift velocity given by equations (29) and (30)? To answer this question, it is desirable to measure the local drift velocity in a large diameter vessel. Figure 6 shows the local drift velocity in air–water two-phase

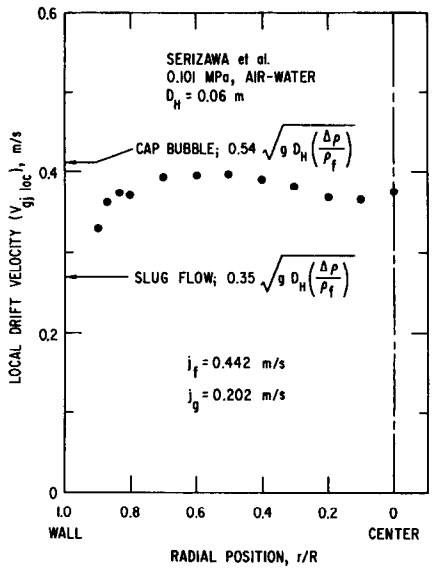

FIG. 6. Experimental data of local drift velocity by Serizawa *et al.* [31–33].

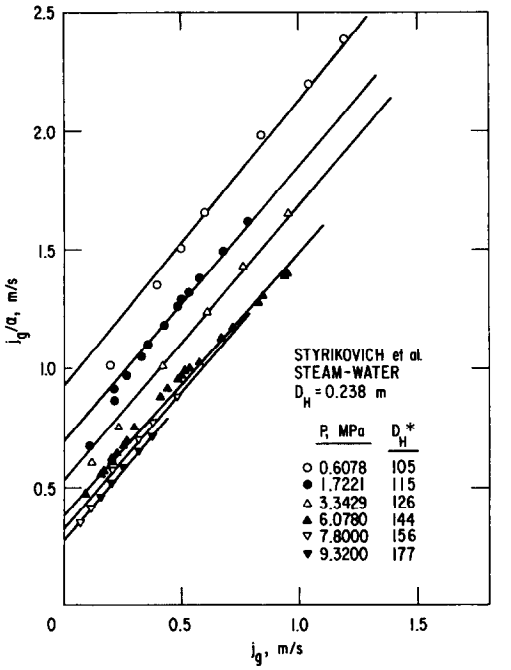

FIG. 7. Experimental data of Styrikovich *et al.* [24] in the j_g vs j_g/α plane.

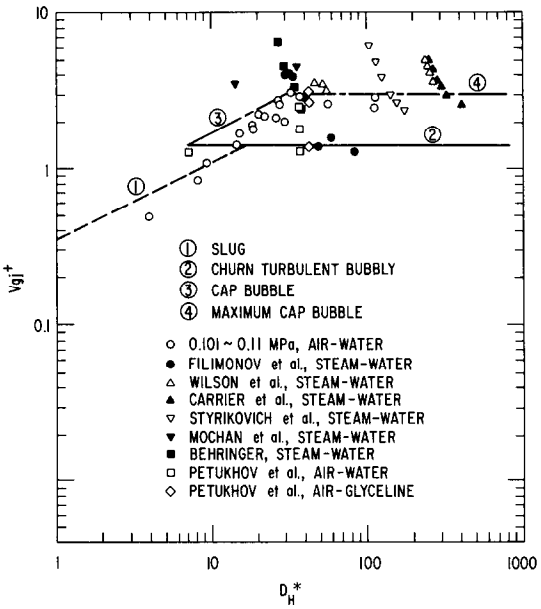

FIG. 8. Drift velocities obtained from various experiments [13, 14, 16–18, 21–24, 26, 27, 33, 34] in the D_H^* vs V_{gj}^+ plane.

flow at atmospheric pressure using a 0.06 m pipe [31–33]. The liquid flux j_f is sufficiently low ($j_f = 0.4\ \mathrm{m\ s^{-1}}$) and the experimental results approximately represent the phenomena in bubbling or pool boiling systems. Visual observation reveals that large deformed bubbles, the diameters of which are close to the vessel diameter, appear in this experiment. As shown in this figure, the local drift velocity is larger than that for slug flow given by equation (20), but approximately agrees with the cap bubble drift velocity given by equation (29).

Equations (29) and (30) are derived under the assumption that the surface of the cap bubble is smooth. In real two-phase flow (Figs. 5 and 6) large bubbles can be highly deformed due to natural turbulences in two-phase flow. However, it is noteworthy that the large bubbles in larger diameter vessels approximately behave like a cap bubble rather than a slug bubble in terms of relative motion between phases. For vessels with a diameter much larger than $40\sqrt{(\sigma/g\Delta\rho)}$, the slug bubbles cannot be sustained due to the interfacial instability and they disintegrate to cap bubbles [30]. Therefore, this observation agrees with the theoretical study.

3.2. *Effect of pressure on drift velocity*

Figure 7 shows one example of the experimental data for steam–water at various pressures. Experimental data are plotted in the j_g vs j_g/α plane and the values of j_g/α at $j_g = 0$ indicates the drift velocity. As shown in this figure, the drift velocity decreases as the pressure increases. Detailed examination of this tendency has been done in ref. [26].

Unfortunately, at high pressure steam–water conditions there are few experimental data with systematic changes over the vessel diameter. However, the existing data indicate that the effect of the vessel diameter is similar to that for air–water tests at atmospheric pressure. Figure 8 shows the drift velocities for steam–water, air–water, air–glyceline systems in the V_{gj}^+ vs D_H^* plane. Here V_{gj}^+ is the dimensionless drift velocity given by

$$V_{gj}^+ = \langle\langle V_{gj}\rangle\rangle \Big/ \left(\frac{\sigma g \Delta\rho}{\rho_f^2}\right)^{1/4} \tag{32}$$

and D_H^* is defined by equation (9). Basically, the drift

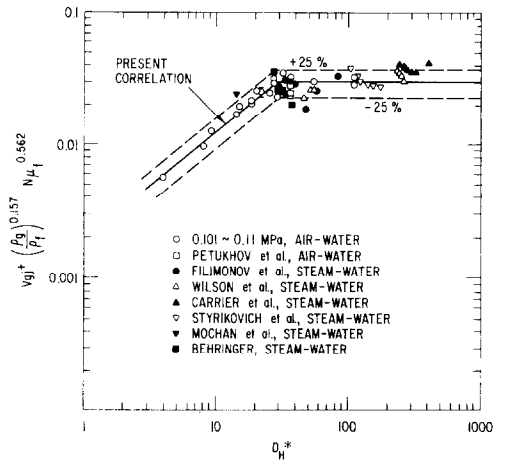

FIG. 9. Comparison of experimental drift velocities for air water and steam–water with values predicted by equations (34) and (35) (present correlation).

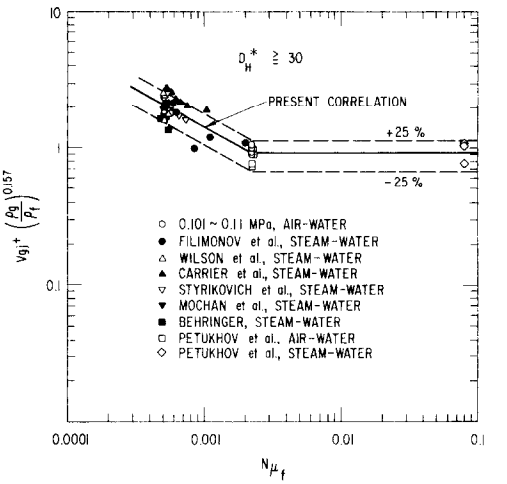

FIG. 10. Comparison of experimental drift velocity for air–water, air–glyceline and steam–water ($D_H^* \geq 30$) with values predicted by equations (38) and (39) (present correlation).

velocity for large diameter vessels shows the trend of the cap bubble drift velocity, equations (29) and (30). However, higher pressure data show considerable scatter. The detailed examination of data [26] indicates that the drift velocity systematically changes with a system pressure. Moreover, the experimental data show that the drift velocities for steam–water, air–water and air–glyceline sysems take different values at the same pressure. This can be attributed to the difference in physical properties in the liquid phase. The drift velocity is closely related to the drag coefficient for bubbles and the drag coefficient depends mainly on the liquid phase properties [4, 36]. In view of the detailed analysis on the drag coefficient fluid particles [4, 36], one may use the viscosity number, $N_{\mu f}$ as a non-dimensional parameter characterizing the liquid phase properties. It is defined by

$$N_{\mu f} \equiv \frac{\mu_f}{\left(\rho_f \sigma \sqrt{\left(\frac{\sigma}{g\Delta\rho}\right)}\right)^{1/2}} \tag{33}$$

where μ_f is the viscosity of a liquid phase.

Using this parameter and density ratio between liquid and gas, the drift velocity is correlated. Figure 9 shows the drift velocity for air–water and steam–water systems ($N_{\mu f} \leq 2 \times 10^{-3}$) at various pressures and various vessel diameters in the

$$V_{gj}^+ \left(\frac{\rho_g}{\rho_f}\right)^{0.157} N_{\mu f}^{0.562} \text{ vs } D_H^* \text{ plane.}$$

The drift velocity is then correlated by

$$V_{gj}^+ = 0.0019 D_H^{*0.809} \left(\frac{\rho_g}{\rho_f}\right)^{-0.157} N_{\mu f}^{-0.562} \quad \text{for} \quad D_H^* \leq 30 \tag{34}$$

$$V_{gj}^+ = 0.030 \left(\frac{\rho_g}{\rho_f}\right)^{-0.157} N_{\mu f}^{-0.562} \quad \text{for} \quad D_H^* \geq 30. \tag{35}$$

These correlations are valid for low viscous fluids satisfying

$$N_{\mu f} \leq 2.2 \times 10^{-3}. \tag{36}$$

Equations (39) and (40) are applicable for the slug flow or cap bubble regime.

Based on the experimental data for the air–glyceline system [29], the effect of viscosity number for large $N_{\mu f}$ can be estimated. Available data for the air–glyceline system is limited for larger diameters only given by

$$D_H^* \geq 30. \tag{37}$$

In Fig. 10, the drift velocities for $D_H^* \geq 30$, are plotted in the

$$V_{gj}^+ \left(\frac{\rho_g}{\rho_f}\right)^{0.157} \text{ vs } N_{\mu f} \text{ plane.}$$

Although the data for large $N_{\mu f}$ are not sufficient, the data show the trend of the effects of $N_{\mu f}$ as (for $D_H^* \geq 30$)

$$V_{gj}^+ = 0.030 \left(\frac{\rho_g}{\rho_f}\right)^{-0.157} N_{\mu f}^{-0.562} \quad \text{for} \quad N_{\mu f} \leq 2.2 \times 10^{-3} \tag{38}$$

$$V_{gj}^+ = 0.92 \left(\frac{\rho_g}{\rho_f}\right)^{-0.157} \quad \text{for} \quad N_{\mu f} \geq 2.2 \times 10^{-3}. \tag{39}$$

The effect of the density ratio and liquid viscosity number on the drift velocity can be attributed to the change in drag coefficient of the cap bubble in two-phase media. When one denotes the drag coefficient for infinite liquid and two-phase media by $C_{D\infty}$ and C_D, they are given in terms of drift velocity by

$$\frac{C_D}{C_{D\infty}} = \left(\frac{V_{gj\infty}}{\langle\langle V_{gj} \rangle\rangle}\right)^2 \tag{40}$$

where $V_{gj\infty}$ is the terminal velocity of a bubble in an

infinite liquid. For example, for a large diameter vessel, $D_H^* \geqslant 30$ and $N_{\mu f} \leqslant 2.25 \times 10^{-3}$, the drift velocity in two-phase media is given by equation (38). On the other hand, $V_{gj\infty}$ is approximately given by equation (30). Substituting equations (38) and (30) into equation (40), one obtains

$$\frac{C_D}{C_{D\infty}} = 10^4 \left(\frac{\rho_g}{\rho_f}\right)^{0.314} N_{\mu f}^{1.124}. \quad (41)$$

In the two-phase flow of a bubbling or boiling pool, large bubbles (slug or cap bubbles) accompany many small bubbles in the liquid slug section [16, 21]. These bubbles affect the drag coefficient of large bubbles. The (ρ_g/ρ_f) term in equation (41) is assumed to represent the effect of small bubbles and other large bubbles. It is also possible that significant droplet entrainment into gas space occurs. This may also explain the effect of the density ratio in the drift velocity correlation.

The viscosity effect term, $N_{\mu f}$, in equation (41) is considered to represent the effect of liquid motion around large bubbles induced by the bubble motion and the interfacial shear between large bubbles and liquid. The dependence of drift velocity on $N_{\mu f}$ as indicated in equation (41) may be attributed to the fact that large bubbles are highly deformed in bubbling and pool boiling in large diameter vessels [16, 21].

3.3. *Distribution parameter*

Besides the average local drift velocity described above, the distribution parameter C_0 in bubbling or pool boiling must be addressed. The distribution parameter reflects the difference in the cross-sectional area averaged velocities of gas and liquid due to the radial distribution of the void and velocity [2, 3, 37]. As described in Section 2.3, the distribution parameter in a forced convection system is given by equations (16) and (17) [3].

In the bubbling and pool boiling system, the distributions of the void fraction and liquid velocity have been measured by some researchers [38–40]. They have reported that there is liquid upflow in the central region and liquid downflow in the outer region. This liquid flow is induced by the bubble motion and affects the distribution parameter. In principle, the distribution parameter can be obtained by measuring the radial distributions of void fraction and velocities of each phase. However, such data have not been obtained in sufficient amounts to develop a correlation for the distribution parameter. Therefore, the distribution parameters in bubbling and pool boiling have been determined by a slope of j_g vs j_g/α relations by assuming C_0 is constant for each set of data as listed in Table 1 [2]. The results are shown in Figs. 11 and 12 (Fig. 11 for round tube and Fig. 12 for rectangular channel). In these figures, Ishii's correlation [3] for the distribution parameter for a forced convection system, equations (16) and (17), are

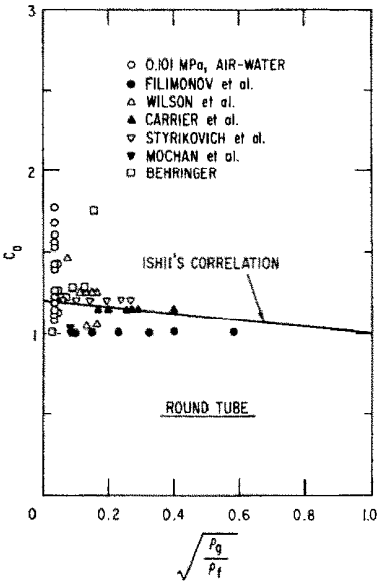

FIG. 11. Distribution parameters for round tube.

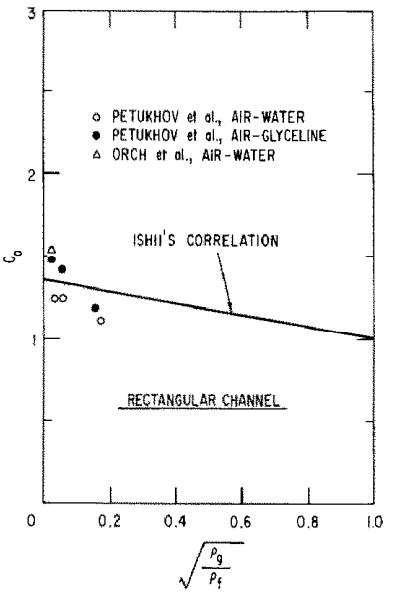

FIG. 12. Distribution parameters for rectangular channel.

shown. The experimentally obtained distribution parameters for bubbling or pool boiling system scatter around equations (16) and (17), and particularly data for a rectangular duct are not sufficient. The large scatters of experimental data can be attributed to several factors. First, due to the relatively large values of the pool diameter to height ratio, the inlet condition plays a very important role in determining the distribution parameter in pool bubbling systems. Second, the distribution parameter appears to be a function of the hydraulic diameter particularly for larger diameters, see Fig. 4. Both of these effects have been neglected in Ishii's correlation for C_0. However, as an average the correlation for forced convection, equations (16) and (17), may approximately be

applied to bubbling or pool boiling systems due to the following reason. For pool bubbling systems, the order of magnitude of the distribution parameter effect and of the local slip effect are about the same. Thus in calculating a void fraction, the value of C_0 is not as critical as in a forced convection system where often C_0 is the dominant factor because of large values of the total flux j. However, for a general correlation, it is necessary to model the distribution factor C_0 more accurately.

4. COMPARISON OF EXPERIMENTAL POOL VOID FRACTION WITH CORRELATION

In the previous sections, new correlations for the average local drift velocity have been developed for pool bubbling systems. The distribution parameter has also been examined in terms of experimental data and a recommended correlation has been given. These are listed below.

Low viscous case: $N_{\mu f} \leqslant 2.25 \times 10^{-3}$

$$V_{gj}^{+} = 0.0019 D_H^{*0.809} \left(\frac{\rho_g}{\rho_f}\right)^{-0.157} N_{\mu f}^{-0.562}$$

for $D_H^* \leqslant 30$

$$V_{gj}^{+} = 0.030 \left(\frac{\rho_g}{\rho_f}\right)^{-0.157} N_{\mu f}^{-0.562} \quad \text{for} \quad D_H^* \geqslant 30.$$

Higher viscous case: $N_{\mu f} > 2.25 \times 10^{-3}$

$$V_{gj}^{+} = 0.92 \left(\frac{\rho_g}{\rho_f}\right)^{-0.157} \quad \text{for} \quad D_H^* \geqslant 30.$$

Distribution parameter

$C_0 = 1.2 - 0.2\sqrt{(\rho_g/\rho_f)}$ for round tube

or

$C_0 = 1.35 - 0.35\sqrt{(\rho_g/\rho_f)}$ for rectangular channel.

Then the pool void fraction can be calculated using equation (22) coupled with correlations for drift velocity and distribution parameter.

Figures 1 and 2 show the comparison of experimental values of the pool void fraction with the present correlation (equation (22) with equations (34), (35), (39), (16) and (17)). The experimental conditions of these figures are summarized in Table 1. In these figures experimental data are plotted in the α vs j_g^+ plane. Detailed comparisons between the present correlation and experimental data as listed in Table 1 have been done in ref. [26].

As shown in these figures, the present correlation can predict the experimental pool void fraction for wide ranges of gas flux, system pressures, vessel diameters and liquid physical properties.

Figures 13 and 14 also show the comparison of the experimental pool void fraction and the pool void fraction predicted by the present correlation. The

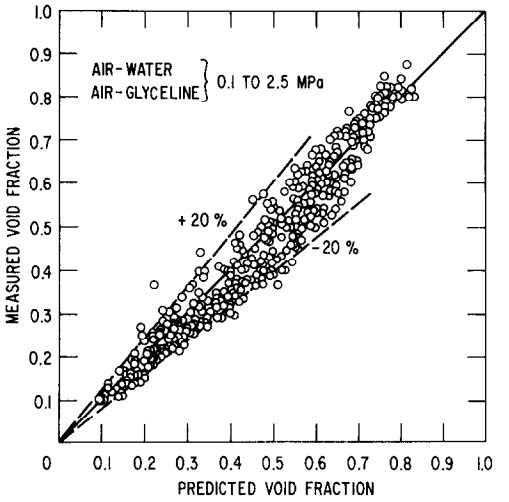

FIG. 13. Comparative representation of experimental and predicted pool void fraction for air–water and air–glyceline [16–18, 21, 26–28].

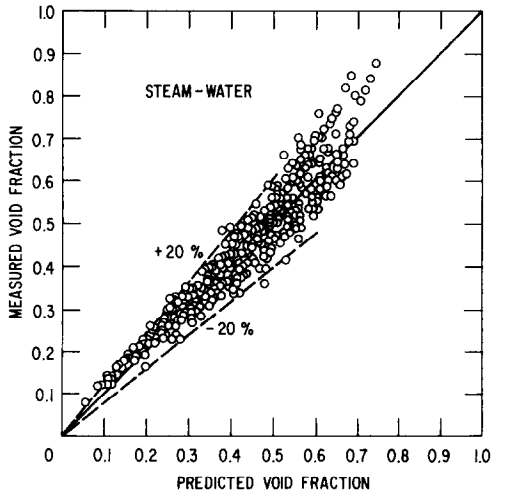

FIG. 14. Comparative representation of experimental and predicted pool void fraction for steam–water [13, 14, 22–24, 33, 34].

experimental conditions of these figures are summarized in Table 1. As shown in these figures the present correlation can predict the experimental data of the pool void fraction within $\pm 20\%$.

As described in Section 1, one of the most important applications of the pool void fraction correlation is to predict the true liquid level in bubbling or pool boiling systems. This prediction can be given by equation (1). In view of equation (1), to predict the true liquid level, the accuracy of the liquid fraction $(1-\alpha)$ is quite important particularly for high void fraction. For Figs. 13 and 14 it can also be seen that the accuracy of the prediction of the liquid fraction is also within $\pm 20\%$. The accuracy is even much higher at lower void fractions.

5. SUMMARY AND CONCLUSIONS

An accurate prediction of the void fraction and relative motion between phases in bubbling or boiling pool is quite important in many engineering systems. Similarly these are also important in relatively large diameter vessels under liquid flowing conditions. There are several empirical correlations for pool void fraction, however it has not been studied from basic physical phenomena involved in the relative motion between phases. In view of the above, an analysis of relative motions between phases has been carried out for low liquid flow cases in relatively large diameter pipes and vessels. First, it was shown that the application of the conventional drift flux model to bubbling or boiling pool was limited to low gas fluxes where $j_g < 0.5(\sigma g \Delta p/\rho_f^2)^{0.25}$. For higher gas fluxes above this limit, a new drift flux model was developed based on the recent theoretical result on the maximum bubble size and experimental data. This phenomenological model was then applied to pool boiling and pool bubbling cases to obtain a new correlation for the pool void fractions. It was shown that the new correlation could be applied to a wide range of gas flux, system pressures, vessel diameters and liquid physical properties. Since the present model has the form of the drift flux model, it can also be applied to pool bubbling cases as well as flowing cases. These are significant improvements over the existing empirical correlation for pool void fractions.

At the higher gas flux range, cap bubbles or slug bubbles dominate the hydrodynamic behavior. Thus the pool void fraction and drift velocity are mainly determined by the rise velocity of these large bubbles. The smaller bubbles are entrained in the wakes of the larger bubbles and rise with them. Another important effect is the formation of the secondary circulation which act as channeling for gas bubbles in a larger diameter pipe. At higher gas fluxes the drift velocity is a strong function of a pipe diameter up to a certain diameter determined by fluid and gas properties. Physically this upper limit on the pipe diameter is determined by the maximum stable cap bubble size given approximately by $30\sqrt{(\sigma/g\Delta\rho)}$. In pipes below this value, the large bubbles are elongated due to the wall effect, and these elongated slug bubbles dominate the relative motion between phases. For pipes having a diameter larger than the above noted limit, the slug bubbles are generally unstable. Therefore, the hydrodynamically most dominant bubbles are the cap bubbles near the maximum stable size.

In addition to the strong relation to the rise velocity of a slug bubble or cap bubble depending on a pipe diameter, the mean local drift velocity correlation showed the effect of the density ratio and liquid viscosity number. These were attributed to the change in the drag coefficient due to the existence of small bubbles, recirculation around large bubbles and interfacial deformation.

The present correlation fits to a large number of experimental data of pool void fraction over wide ranges of gas flux (10–250 cm s^{-1}), vessel diameter (1–60 cm) and system pressure (0.1–2.5 Mpa for air–water and 0.1–18.2 MPa for steam–water). The accuracy of the prediction of void fraction and liquid fraction is within $\pm 20\%$.

However, it should be noted that the distribution parameter for relatively large pipes at low liquid flow rates showed considerable scatters when it was compared to the forced flow correlation developed by Ishii. These can be attributed to several factors. First, the inlet condition plays a very important role in determining the phase distribution at low liquid flow in relatively large diameter and short pipes. The pool bubbling experiment data falls in this category. Second, the distribution parameter appears to be a function of the hydraulic diameter particulary for larger diameters due to the recirculation flow. Both of these effects have been neglected in Ishii's correlation which were developed for fully developed flow in relatively small pipes. For pool void fraction the effect of the distribution parameter is relatively small compared with the mean local drift velocity because the total volumetric flux is small. Therefore, the model fits well with the data, however, for a general correlation it is necessary to model the distribution parameter more accurately. For this purpose, experimental data for void and velocity profiles in relatively large diameter pipes (> 10 cm) are required.

Acknowledgment—A part of this study is performed under the auspices of the U.S. Nuclear Regulatory Commission. The authors would like to thank Drs N. Zuber and R. Lee of NRC for their support.

REFERENCES

1. I. Kataoka and M. Ishii, Mechanistic modeling and correlation for pool entrainment phenomenon, *Int. J. Heat Mass Transfer* **27**, 1999–2014 (1984).
2. N. Zuber and J. A. Findlay, Average volumetric concentration in two-phase flow systems, *Trans. Am. Soc. Mech. Engrs J. Heat Transfer* **87**, 453 (1965).
3. M. Ishii, One-dimensional drift-flux model and constitutive equations for relative motion between phases in various flow regimes, Argonne National Laboratory Report ANL-77-47 (1977).
4. M. Ishii and N. Zuber, Drag coefficient and relative velocity in bubbly, droplet or particulate flows, *A.I.Ch.E. Jl* **25**, 843 (1979).
5. G. B. Wallis, *One-dimensional Two-phase Flow*, Chap. 4. McGraw-Hill, New York (1969).
6. M. Ishii, *Thermo-fluid Dynamic Theory of Two-phase Flow*. Eyrolles, Paris, France (1975).
7. M. Ishii and K. Mishima, Study of two-fluid model and interfacial area, Argonne National Laboratory Report ANL-80-111, NUREG/CR-1873 (1980).
8. J. M. Delhaye, Equations fondamentales des ecoulements diphasiques, Part 1 and 2, CEA-R-3429, France (1968).
9. G. C. K. Yeh and N. Zuber, On the problem of liquid entrainment, Argonne National Laboratory Report ANL-6244 (1960).
10. L. S. Sterman, The generalization of experimental data concerning the bubble of vapor through liquid, *J. Tech.*

Phys. (*U.S.S.R.*) **26,** 1519 (1956).
11. B. A. Dimentiev, R. S. Lepilin and A. A. Loginov, An investigation of hydrodynamic process of bubbling through a vapor liquid mixture of considerable height, *Nauch. Dokl. Vish. Shkol-Energetica* No. 2, 251 (1959) (quoted from ref. [9]).
12. L. S. Sterman, The theory of steam separation, *J. Tech. Phys.* (*U.S.S.R.*) **28**(7), 9 (1958).
13. J. F. Wilson, R. J. Grenda and J. F. Patterson, Steam volume fraction in a bubbling two-phase mixture, *Trans. ANS* **4,** 356 (1961).
14. J. F. Wilson, R. J. Grenda and J. F. Patterson, The velocity of rising steam in a bubbling two-phase mixture, *Trans. ANS* **5,** 151 (1962).
15. G. G. Bartolomei and M. S. Alkhuton, Determination of the true vapor content when there is bubbling in the stabilization section, *Teploenergetika* **14**(12), 80 (1967).
16. Y. Sudo, Estimation of average void fraction in vertical two-phase flow channel under low liquid velocity, *J. Mech. Sci. Technol.* **17**(1), 1 (1980).
17. R. V. Baily, P. C. Zmola, F. M. Taylor and R. J. Planchet, Transport of gases through liquid–gas mixture, paper presented at the AIChE New Orleans Meeting (1956) (quoted from ref. [2]).
18. K. W. Orth, Hydrodynamic aspects of volume boiling, M.S. thesis, Marquette University, Mech. Engng Dept. (1980).
19. N. Zuber and J. Hench, Steady-state and transient void fraction of bubbling systems and their operating limits, General Electric Report 62GL100 (1962).
20. G. B. Wallis, *One-dimensional Two-phase Flow*, p. 263. McGraw-Hill, New York (1969).
21. K. Yamaguchi and Y. Yamazaki, Characteristics of countercurrent gas–liquid two-phase flow in vertical tubes, *J. Nucl. Sci. Technol.* **19**(12), 985 (1982).
22. F. Carrier *et al.*, Steam separation technology under the Euroatom Program, Allis–Chalmers Atomic Energy Div., Report No. ACNP-63021 (1963) (quoted from ref. [2]).
23. A. I. Filimonov, M. M. Przhizhalovski, E. P. Dik and J. N. Petrova, The driving head in pipes with a free interface in the pressure range from 17 to 180 atm, *Teploenergetika* **4,** 22 (1957).
24. M. A. Styrikovich, A. V. Surnov and J. G. Vinokour, Experimental data on hydrodynamics of two-phase mixture, *Teploenergetika* **8,** 56 (1961).
25. D. A. Labuntov, I. P. Kornyukhin and E. A. Zakharova, Vapor concentration of a two-phase adiabatic flow in vertical ducts, *Teploenergetika* **15**(4), 62 (1968).
26. I. Kataoka and M. Ishii, Prediction of pool void fraction by new drift flux correlation, Argonne National Laboratory Report NUREG/CR-4657, ANL-86-29 (1986).
27. J. E. Ellis and E. L. Jones, Vertical gas–liquid flow problems, Symposium on Two-phase Flow, Exter. B101-140, 21–23 June (1965).
28. G. E. Smissaert, Two-component two-phase flow parameters for low circulation rate, Argonne National Laboratory Report ANL-6755 (1963).
29. V. I. Petukhov and V. A. Kolokoltsen, Effect of liquid viscosity on droplet entrainment and volumetric air content, *Teploenergetika* **12**(9), 30 (1965).
30. M. Ishii and G. Kocamustafaogullari, Private communication (1984). Also Maximum fluid particle size for bubbles and drops, ASME Winter Annual Meeting, *Proc. "Fundamental Aspects of Gas–Liquid Flow"*, FED-vol. 29, p. 99. Miami Beach, Florida, 17–22 Nov. (1985).
31. A. Serizawa, I. Kataoka and I. Michiyoshi, Turbulence structure of air–water bubbly flow, I. Measuring techniques, *Int. J. Multiphase Flow* **2,** 221 (1975).
32. A. Serizawa, I. Kataoka and I. Michiyoshi, Turbulence structure of air–water bubbly flow, II. Local properties, *Int. J. Multiphase Flow* **2,** 235 (1975).
33. A. Serizawa, I. Kataoka and I. Michiyoshi, Turbulence structure of air–water bubbly flow, III. Transport properties, *Int. J. Multiphase Flow* **2,** 247 (1975).
34. P. Behringer, Steiggeshurndigkeit von Dampfblasen in Kesselrohrev, *VDI ForschHft* **365** (1934).
35. Mochan *et al.*, *Énergomashinostroenic* No. 5 (1956) (quoted from ref. [23]).
36. M. Ishii and T. C. Chawla, Local drag laws in dispersed two-phase flow, Argonne National Laboratory Report ANL-79-105, NUREG/CR-1230 (1979).
37. S. G. Bankoff, A variable density single-fluid model for two-phase flow with particular reference to steam–water flow, *Trans. Am. Soc. Mech. Engrs J. Heat Transfer* **82,** 265 (1965).
38. J. H. Hills, Radial Non-uniformity of velocity and voidage in a bubble column, *Trans. Instn Chem. Engrs* **52,** 1 (1974).
39. V. P. Pavlov, Circulation of fluid in bubbling apparatus of periodical operation, *Khim. Prom.* No. 9, 698 (1965).
40. N. de Nevers, Bubble driven fluid circulations, *A.I.Ch.E. Jl* **14**(2), 222 (1968).

MODELE DE FLUX D'ENTRAINEMENT POUR DE GRANDS DIAMETRES DE TUBE ET FORMULES NOUVELLES POUR FRACTION DE VIDE EN RESERVOIR

Résumé—La fraction de vide pour un système à bouillonnement de bulles ou en ébullition est un des paramètres importants dans l'analyse des mécanismes de transfert de chaleur et de masse. En utilisant la formulation de flux d'entrainement, des formules pour la fraction de vide ont été obtenues en s'appuyant sur un grand nombre de données expérimentales. On trouve que la vitesse d'entrainement dans un système en réservoir dépend du diamètre du récipient, de la pression du système, du flux gazeux et des propriétés physiques du fluide. Les résultats montrent que la vitesse relative et la fraction de vide peuvent être complètement différentes de celles prédites par des formules conventionnelles. En terme de vitesse d'ascension, quatre régimes différents sont identifiés. Les formules actuelles s'accordent avec les données expérimentales dans un large domaine de paramètres tels que diamètre du récipient, pression du système, flux gazeux et propriétés physiques.

EIN DRIFT-GESCHWINDIGKEITS-MODELL FÜR ROHRE MIT GROSSEM DURCHMESSER UND EINE NEUE KORRELATION FÜR DEN GASGEHALT IN BEHÄLTERN

Zusammenfassung—Der Gasgehalt eines in einem Behälter siedenden oder von Blasen durchströmten Systems ist einer der wichtigen Parameter bei der Untersuchung von Wärme- und Stoffübertragungsprozessen. Mit Hilfe des Drift-Geschwindigkeits-Modells und unter Verwendung einer großen Anzahl von experimentellen Daten wurden Korrelationen für den Gasgehalt in einem Behälter aufgestellt. Es wurde festgestellt, daß die Drift-Geschwindigkeit in einem Behälter von dem Behälterdurchmesser, dem Systemdruck, dem Gasdurchsatz und den physikalischen Eigenschaften des Fluids abhängig ist. Die Ergebnisse zeigen, daß sich bei der Relativgeschwindigkeit und beim Gasgehalt Abweichungen von den Werten, die mit herkömmlichen Korrelationen berechnet wurden, ergeben. In Abhängigkeit der Aufstiegsgeschwindigkeit wurden vier Bereiche unterschiedlicher Blasenform erkannt: Kugelblasen, Ellipsoidblasen mit innerer Zirkulation, Pilzblasen und Schirmblasen. Die vorgestellten Korrelationen stimmen mit den experimentellen Daten in einem weiten Parameterbereich wie Behälterdurchmesser, Systemdruck, Gasdurchsatz und Stoffeigenschaften überein.

ИССЛЕДОВАНИЕ ТЕПЛО-И МАССООБМЕНА В ТРУБАХ БОЛЬШОГО ДИАМЕТРА С ПОМОЩЬЮ МОДЕЛИ СПУТНОГО ПОТОКА. НОВОЕ КРИТЕРИАЛЬНОЕ СООТНОШЕНИЕ ДЛЯ ОБЪЕМНОГО ПАРОСОДЕРЖАНИЯ

Аннотация—Показано, что объемная доля пузырей при барботаже и паросодержание при кипении системы является одним из важнейших параметров при исследовании процессов тепло-и массообмена. С помощью модели спутного потока на основании большого количества экспериментальных данных получены критериальные соотношения для объемного паросодержания. Найдено, что скорость спутного потока в объеме зависит от диаметра сосуда, общего давления и физических свойств газа и жидкости. Результаты исследования показывают, что относительная скорость и паросодержание могут отличаться от их значений, рассчитанных с помощью традиционных соотношений. В зависимости от скорости подъема пузырьков установлены четыре различных режима течения: пузырьковый, турбулентно-вспенивающий, стержневой и режим колпачковых пузырьков. Показано, что предлагаемые соотношения хорошо коррелируют с экспериментальными данными в широком диапазоне изменения параметров, таких как диаметр сосуда, общее давление, газовый поток и физические свойства жидкости.